

# Structural evolution of the Precambrian Bjerkreim–Sokndal intrusion, South Norway

JOHANNE PALUDAN, ULLA B. HANSEN & NIELS Ø. OLESEN

Paludan, J., Hansen, U. B. & Olesen, N. Ø.: Structural evolution of the Precambrian Bjerkreim–Sokndal intrusion, South Norway. *Norsk Geologisk Tidsskrift*, Vol. 74, pp. 185–198. Oslo 1994. ISSN 0029-196X.

The structures of the northwestern part of the Precambrian Bjerkreim–Sokndal intrusion are studied from micro- to macro-scale. Meso-scale structures are dominated by (1) modal layering of igneous origin ( $S_0$ ), and (2) prominent linear and planar fabrics ( $L_1/S_1$ ), defined by the shape-preferred orientation of minerals and mineral aggregates. In most places  $S_0$  and  $S_1$  are parallel, and together they define an isoclinal syncline with a southeastwards plunging fold axis. The linear fabric ( $L_1$ ) is subparallel to the fold axis in the hinge zone and converges towards this zone in the limbs. The intensity and type of fabric vary across the fold. In the hinge zone the L-fabric is dominant, whereas the rocks in the limbs display a combined S- and L-fabric. The intensity of the fabric is closely tied with microstructural indications of plastic deformation, such as lattice bending and kinking, polygonization and recrystallization. All of this points to one major phase of solid state deformation. Estimates of the strain state are based on regional variations in the shape of olivine grains and aggregates from two igneous units. Extensions of up to about 100% are observed in the hinge zone, and flattening around 40% is observed in the southern limb. Rheological considerations suggest that these are minimum values. In our interpretation, the deformation was the result of passive subsidence of the intrusive rocks, induced by gravitational instabilities in the area (inverse diapirism). A convergent flow pattern led to the formation of L-tectonites in the hinge zone and an additional shear component along the limbs led to the formation of L/S-tectonites. A series of monzonitic dykes (the Lomland dykes) and a number of minor shear zones all post-date the major deformation. The dykes and shear zones may be coeval.

Johanne Paludan, Ulla B. Hansen & Niels Ø. Olesen, Department of Earth Sciences, Aarhus University, C. F. Møllers Allé, DK-8000 Århus C, Denmark.

## Introduction

The Bjerkreim–Sokndal (BKSK) intrusion is a layered mafic body which crops out about 50 km southeast of Stavanger, South Norway (Fig. 1). It belongs to the huge 'South Rogaland Igneous Province' which consists of a suite of rocks of Precambrian age, including massif type anorthosites, norites, mangerites, monzonites and charnockites (e.g. Michot 1960; Michot & Michot 1969). Numerous studies of the igneous petrology and magmatic evolution of the intrusive rocks of the province have been conducted (Maijer & Padget 1987; and references therein). There have been recent studies of the BKSK intrusion by Duchesne (1987), Duchesne & Hertogen (1988), Nielsen & Wilson (1991), Nielsen (1992) and Jensen et al. (1993).

The igneous rocks were emplaced into high-grade metamorphic gneisses of dominantly charnockitic composition. The structure of these rocks has been described by Hermans et al. (1975) who found evidence of at least four phases of folding, the most important of which is dominated by north- or northwest-trending, eastward-dipping axial surfaces. The metamorphic evolution and isotope geochronology of the area have been described by, e.g., Hermans et al. (1975), Versteve (1975), Pasteels et al. (1979), Wielens et al. (1980), Wilmart & Duchesne (1987), Maijer (1987) and Duchesne et al. (1993). Four or five phases of metamorphism can be traced, among which the most important events in the BKSK area are (1) a phase of extremely high-temperature granulite fac-

ies (M2) which is generally considered to be related to the emplacement of the igneous province, and (2) a later phase of lower temperature granulite facies metamorphism (M3). Datings typically yield ages of ~1050 Ma for the M2 phase and ~950 Ma for the M3 phase (Maijer 1987).

A suite of massif type anorthositic bodies is present to the southwest of the BKSK intrusion. The largest of these is the Egersund–Ogna body, which is assumed to have been emplaced by a process of solid state doming or diapirism (Michot 1965; Michot & Michot 1969; Maijer & Padget 1987). The occurrence of anorthositic xenoliths in the BKSK intrusion indicates that the massive anorthosites crystallized before the emplacement of the BKSK body. The age of emplacement of the BKSK intrusion may be correlated with the M2 metamorphism (Maijer 1987). However, Pasteels et al. (1979) set the age to  $955 \pm 8$  Ma based on U–Pb dating of a monazite from the gneissic country rocks close to the intrusion contact. Recent age determinations of anorthosites by Duchesne et al. (1993) yield U–Pb ages of ~930 Ma. Thus there is still some confusion regarding the true age of emplacement and crystallization of the BKSK intrusion.

The intrusion is cut by a number of dykes of largely monzonitic composition (the Lomland dyke system) which are related to the smaller Eia–Rekefjord intrusion (Fig. 1). These rocks have been dated to  $946 \pm 14$  Ma, based on a single zircon (Pasteels et al. 1979). Related rocks yield ages of ~920 Ma according to Duchesne et al. (1993).

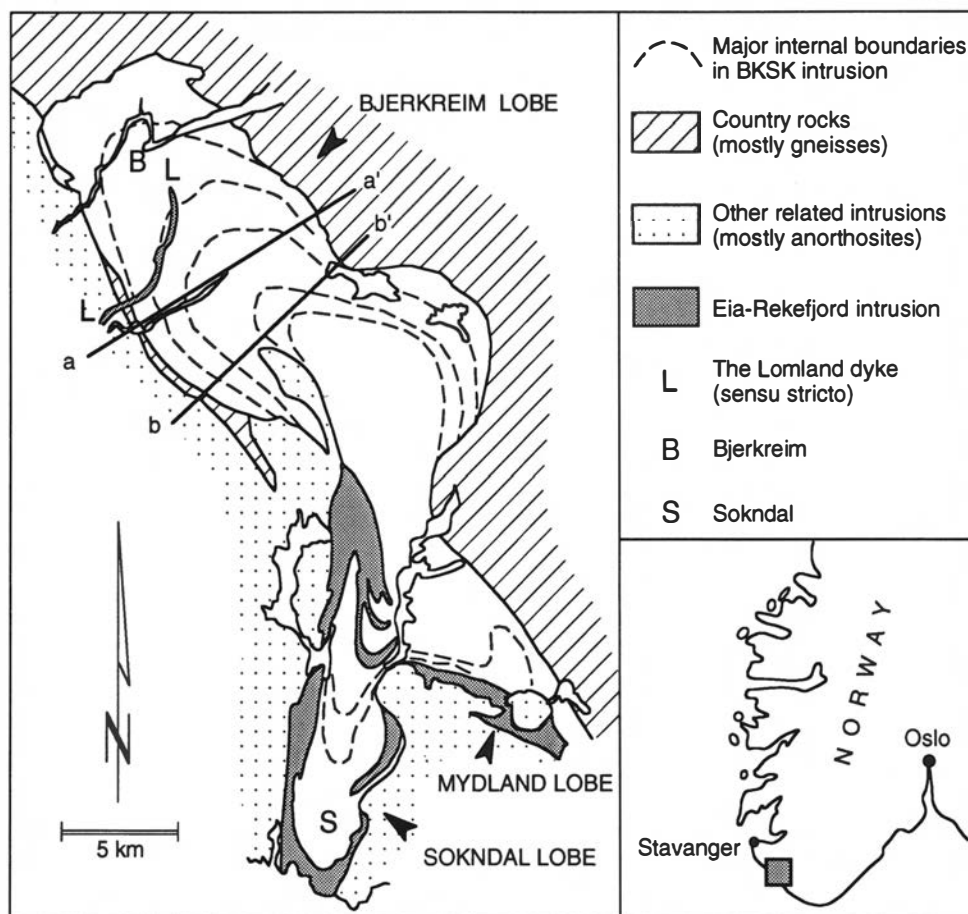


Fig. 1. Outline of the Bjerkreim-Sokndal intrusion, after Duchesne (1987) and Nielsen (1992).

The northwestern lobe of the BSKS intrusion (the Bjerkreim lobe, Fig. 1) is the subject of this study. Towards the southeast similar rocks are exposed in the smaller Sokndal and Mydland lobes. In the Bjerkreim lobe, anorthosite constitutes the northwestern end which is also the stratigraphic and structural base. Towards the southeast follows a several kilometres-thick layered sequence dominated by leuconorites, norites and gabbronorites which form a well-documented igneous stratigraphy (e.g. Nielsen & Wilson 1991). This series contains two approximately 75-m-thick units in which olivine rather than orthopyroxene is the most important mafic phase. These two units of dominantly troctolitic rocks will receive particular attention below. Finally, mangerites and quartz-mangerites are exposed towards the southeast, at the highest stratigraphic and structural level.

At the time of crystallization the igneous layering was close to horizontal. However, towards the top of the layered series variations in the thicknesses of minor units across the intrusion show that the magma chamber floor was subsiding to form a gentle trough shape at the time of crystallization of these units (Nielsen & Wilson 1991). At present the Bjerkreim lobe forms a major syncline and it has been known for a long time that the rocks suffered an event of penetrative deformation (the 'protoclastic deformation' of Michot 1960, 1965; Majer 1987). However, it has been a matter of debate as to whether the penetrative deformation is the result of magmatic flow

processes (as believed by Michot 1960) or a solid state overprinting of local or regional extent. In the interpretation of Hermans et al. (1975) the syncline is coeval with the dominant system of folds in the country rocks.

In this article we report the results of a micro- to macro-scale structural study of the rocks of the Bjerkreim lobe. We attempt to evaluate the magnitude and type of strain which the various parts of the intrusion have experienced, and to establish a history of events, including formation of minor structures and emplacement of the related Lomland dykes.

## Structural elements

### Modal layering

Modal layering forms a prominent planar structure ( $S_0$ ) in large parts of the area, particularly in the noritic and gabbronoritic rocks (Fig. 2A). The layering consists of alternating mafic and felsic bands with an abundance of thin mafic layers, rich in orthopyroxene and Fe-Ti oxide minerals. These layers are 1–10 cm thick and their frequency varies from a few layers to (more rarely) more than 10 layers/m. Modal layering is not developed in the anorthosites and mangerites. Many examples of primary magmatic structures such as impact structures around xenoliths, slump and trough structures, etc., are developed in the modally layered rocks.

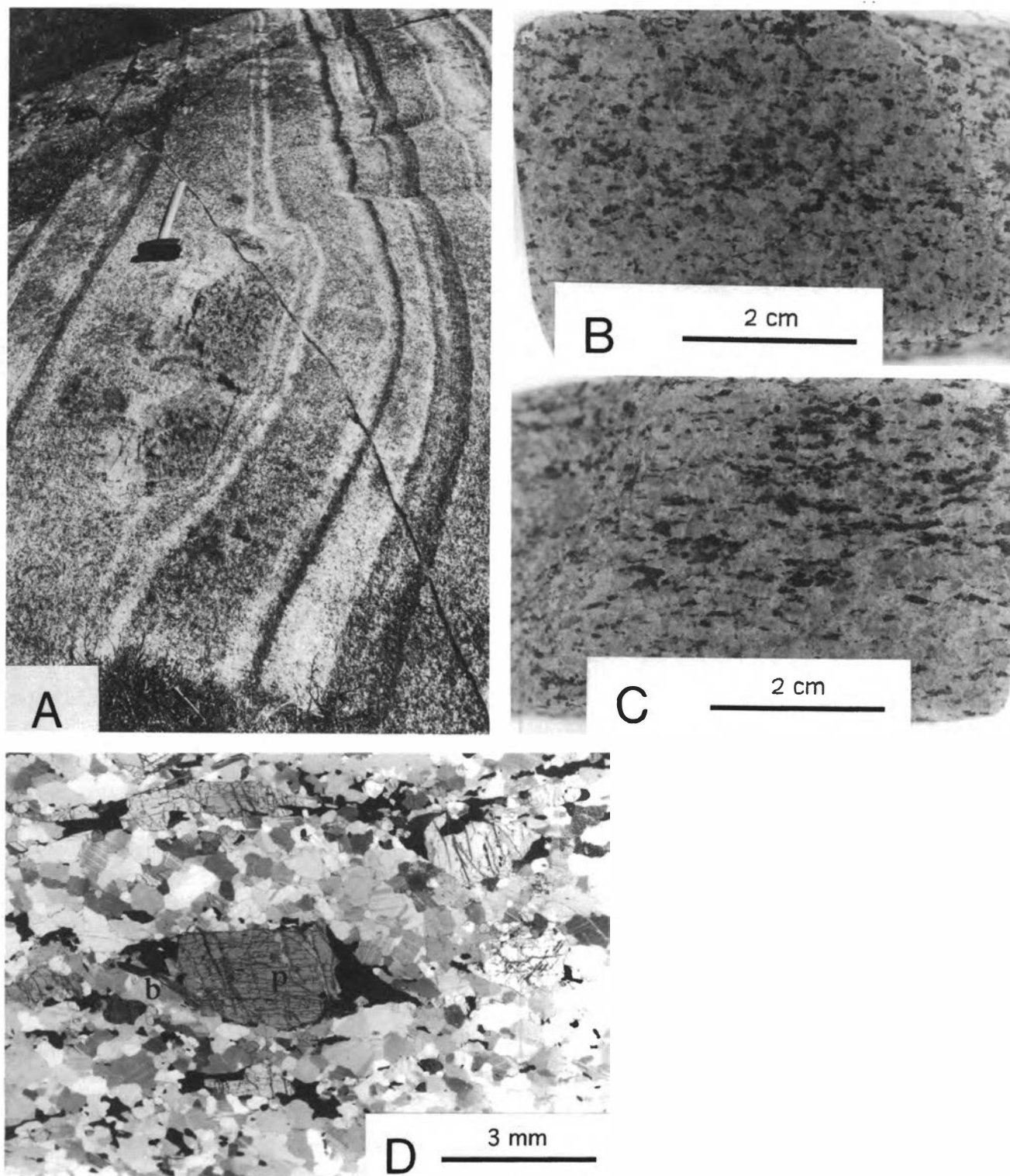


Fig. 2. A: Prominent modal layering ( $S_0$ ) and a xenolith in noritic rocks from the southern limb near Storeknuten (Fig. 4; UTM 34.6/90.5). Younging direction to the left. B & C: Sections through norite specimen from the southern limb at Lake Hellersvatnet (Fig. 4; UTM 37.3/88.8), demonstrating the shape-preferred orientation of minerals and mineral aggregates ( $L_1/S_1$ ). Section B is perpendicular to foliation and lineation and section C is perpendicular to foliation and parallel to lineation. D: Micrograph of leuconorite from the northern limb at Slettebø (Fig. 4; UTM 39.4/95.1), demonstrating pressure shadow-like textures of oxides (black) and biotite (b) around orthopyroxene (p). Section is perpendicular to foliation and parallel to lineation. Note fully recrystallized plagioclase matrix with signs of lattice strain such as bent twin lamellae. Partly crossed polarizers.

#### *Foliation and lineation*

In large parts of the area the rocks display a prominent linear and planar fabric ( $L_1/S_1$ ) defined partly by a shape-preferred orientation (SPO) of the constituent

minerals, in particular pyroxene and plagioclase, and partly by elongate aggregates of mafic minerals, typically pyroxene or olivine, Fe-Ti oxides and sometimes minor amphibole or biotite (Figs. 2B–D). In areas where the

igneous texture is well preserved plagioclase laths occasionally define a primary igneous foliation (lamination). This is most common in the anorthositic rocks at the base of the intrusion. The planar fabric ( $S_1$ ) is generally, but not always, parallel to the modal layering. Aggregates of mafic minerals commonly display a 'pressure shadow-like' texture, in which oxide and occasionally biotite form 'wings' on pyroxene and/or olivine grains (Fig. 2D). In a number of cases these textures are asymmetrical, indicating a non-coaxial strain path.

The deformed igneous rocks are thus generally L/S tectonites (e.g. Twiss & Moores 1992) and the intensity of the fabric is taken as a first approximation of the amount of strain which the rocks have suffered.

### *Major structure*

Mapping of planar structures ( $S_0$ ) in the Bjerkreim lobe reveals the shape of a major isoclinal syncline, whose axis plunges roughly  $35^\circ$  towards the southeast (Figs. 3A, 4, 5 and 6). Both  $S_0$  and  $S_1$  are almost vertical in both limbs and locally overturned in the northern limb east of Lake Teksevatnet. Dips of approximately  $30^\circ$  are observed in the stratigraphically lower part of the hinge zone, gradually increasing to  $40$ – $45^\circ$  at higher levels. Best fit great circle constructions from orientation data yield a fairly constant orientation of the fold axis (Fig. 5). The direction varies from  $123$  to  $128^\circ$ , and the plunge increases from  $32$  to  $43^\circ$  towards the southeast. On the map the trace of the axial surface curves from an orientation of approximately  $140^\circ$  in the northwest to approximately  $120^\circ$  in the southeast (Fig. 3). This corresponds to an axial surface which dips  $80$ – $85^\circ$  towards the northeast in the northwestern part, and is nearly vertical in the southeast.

Overturning of layering in the northern limb appears preferentially in the leuconoritic rocks, whereas layering close to the margin of the intrusion and in the country rock is vertical (Fig. 3A). This indicates that the margin was approximately horizontal prior to folding, whereas the layering was sloping towards the south (i.e. towards the centre of the magma chamber). Thus the major structure is that of an upright to steeply inclined isoclinal fold with a gently curving axial surface. Extrapolation of surface data indicates that the margin (floor) of the intrusion has maximum depths of approximately  $5.5$  km at cross-section aa' of Fig. 1, and  $9$  km below the most westerly part of the mangeritic rocks (cross-section bb' and front section of Fig. 6). The boundary between the anorthosites and the layered rocks is at maximum depths of approximately  $4$  km at cross-section aa' and  $7.5$  km at bb' (Fig. 6).

Smithson & Ramberg (1979) studied the gravity anomaly formed by the intrusion along a line corresponding roughly to cross-section bb'. They interpreted the shape of the intrusion as a gently to moderately inclined syncline of high density (leuconoritic) rocks to a depth of  $4$  km. The lowermost leuconoritic rocks have a relatively

low content of mafic minerals and probably have a density near that of the anorthositic rocks. Therefore the depth calculated by Smithson & Ramberg (1979) is not seriously inconsistent with that indicated by the present knowledge of surface geometry. On the other hand, the inclined shape of the gravity model is not indicated by the orientation of the layering observed at the surface. This implies that the intrusion may deviate considerably from a simple cylindrical shape below the present level of erosion, as shown by the dashed line on Fig. 6.

Minor folds, visible on outcrop scale, are very few. On a larger scale, detailed mapping of the orientation of layering and foliation reveals local deviations from the dominant orientation which in some cases may be due to folding with amplitudes in the  $200$ – $500$  m scale. An example of such a structure is in the hinge zone north-west of Hettebökknuten (Fig. 4; UTM 35.3/95.8).

### *Regional variation of L/S tectonites*

A prominent SPO-defined foliation ( $S_1$ ) is visible in both limbs of the syncline (Figs. 3A and 4). Towards the hinge zone the intensity of the foliation decreases gradually until the rocks are dominantly L-tectonites (i.e. lineated but not foliated, see below). In the leuconoritic and troctolitic rocks the foliation is generally parallel to the modal layering, so that both layering and foliation define the major syncline. However, exceptions to parallelism are observed locally and are well developed in parts of the southern limb, where angles as large as  $20$ – $30^\circ$  between the two planar structures can be observed (Fig. 7).

An equally prominent SPO-defined lineation ( $L_1$ ) is developed in the entire study area with the exception of some massive rocks in the lower anorthositic unit and parts of the stratigraphically lower troctolite unit. In most of the Bjerkreim lobe the lineation plunges gently to moderately southeastwards (Fig. 3B). In the hinge zone immediately surrounding the trace of the axial surface (subareas 4 and 7) the orientation is roughly parallel to the regional fold axis (Figs. 3B, 4 and 5), with a steepening plunge towards the southeast. Towards the southern limb (subarea 3) the orientation gradually shifts towards the east, whereas in the northern limb (subarea 9) it shifts towards a very steep southern plunge. The general pattern is a convergence of the lineations towards a point located in the southeastern part of the area beneath the quartz-mangeritic rocks. In the southern limb (subarea 6) the convergent pattern is less prominent than in the remaining part of the studied area.

The lineations are generally very weak in the structurally lower part of the hinge zone (subareas 1 and 2), moderate in the intermediate part (subareas 3, 4 and 5) and very intense at the highest level of the layered rocks (subarea 7 and parts of 8). Lineations are present in the mangeritic and quartz-mangeritic rocks but are considerably weaker than in the layered rocks immediately below. The shifts in intensity are gradual, with the exception of

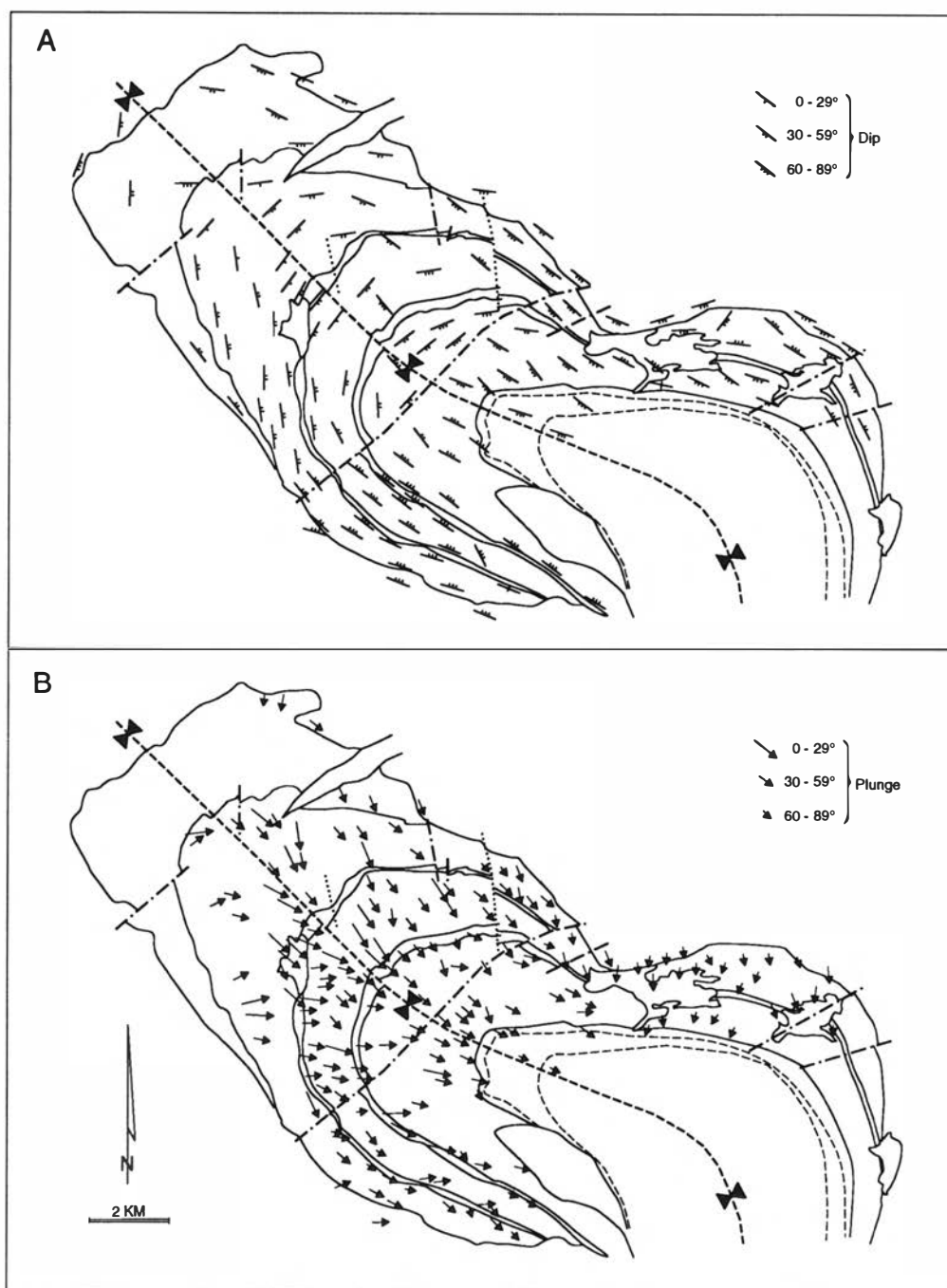


Fig. 3. Representative orientations of fabric elements in the Bjerkreim lobe. A: Planar fabric ( $S_1$ ); B: Linear fabric ( $L_1$ ). For general explanations of the map, see Fig. 4.

the boundary between moderately and intensely lineated rocks, which appears to be related to the Helleland fault, running roughly perpendicular to the axial surface of the syncline along the valley separating subareas 3, 4 and 5 from subareas 6, 7 and 8 (Figs. 3 and 4). Following a particular igneous unit along the strike from the hinge zone towards the limbs, the intensity of both lineation and foliation gradually increases. In the limbs the fabric intensity is relatively constant throughout the layered rocks.

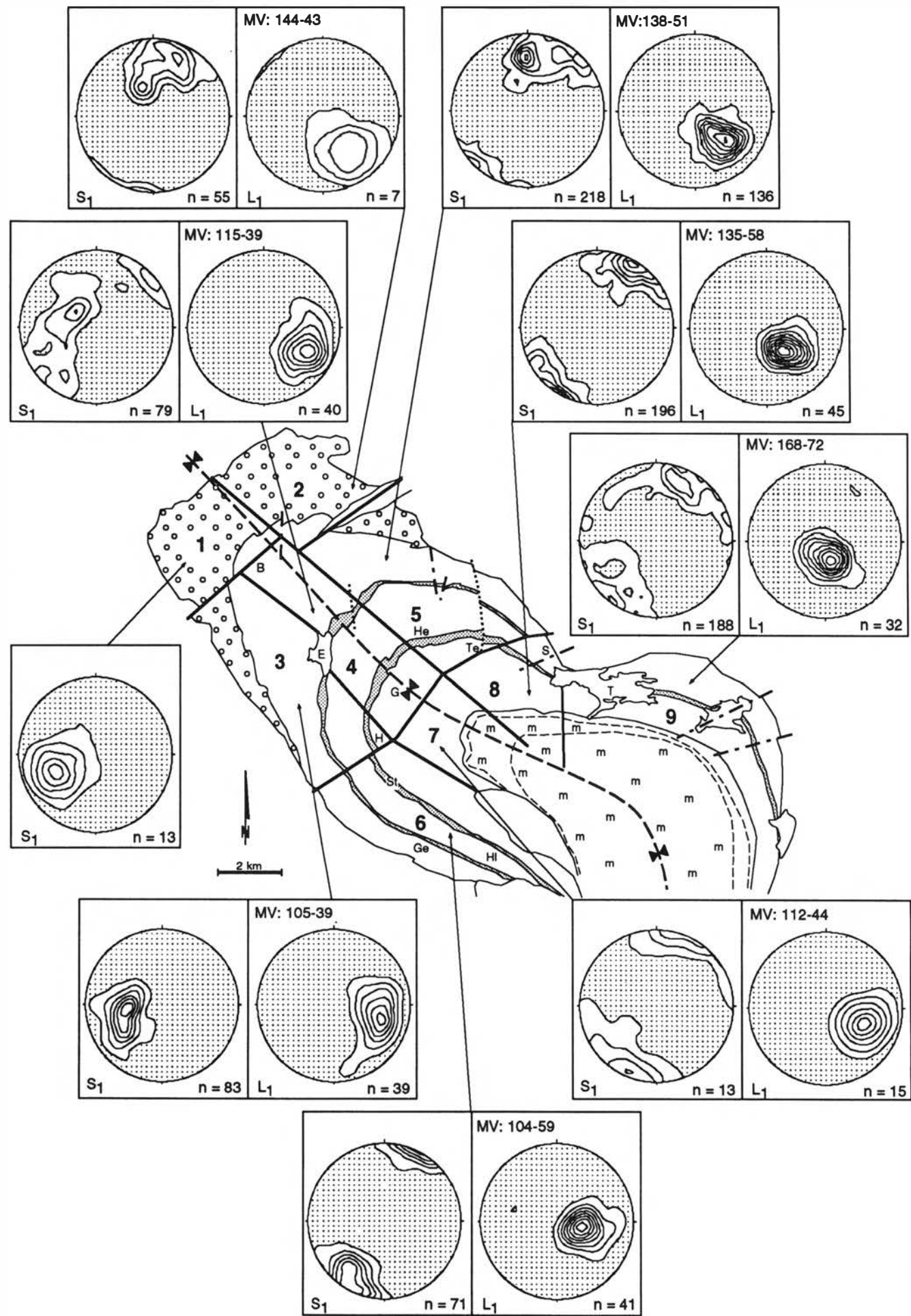
A conspicuous difference in fabric development is observed between the rocks of the troctolite units and the surrounding leuconorites in the area from Helleland to Lake Teksevatnet (subareas 3, 4, 5 and 8; Figs. 4 and 8).

In this area the troctolites are L-tectonites, whereas the leuconorites in subareas 3, 5 and 8 are L/S-tectonites. In subarea 4 the stratigraphically lower troctolite unit has an isotropic fabric whereas the surrounding leuconorites are L-tectonites.

Many xenoliths are present in the study area (Fig. 2A), and it is noteworthy that the SPO-defined fabrics ( $L_1/S_1$ ) continue unbroken through these bodies, indicating that the fabric is strain-related. Likewise, foliations and lineations observed in the country rocks immediately outside the intrusion are concordant with those of the intrusion (Fig. 3).

Microscopical indications of plastic deformation, such as lattice-bending, -kinking and polygonization, are nu-





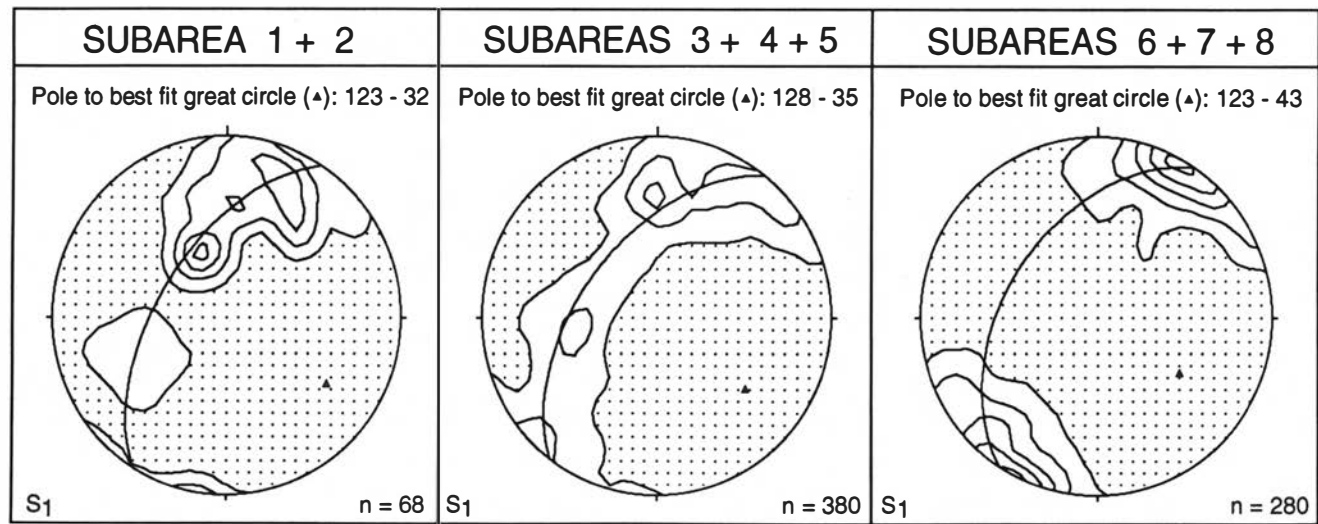


Fig. 5. Orientation of regional fold axis (best fit great circle), constructed from the orientation of planar fabrics (S<sub>1</sub>), in three zones across the fold. Stereographic projections as in Fig. 4.

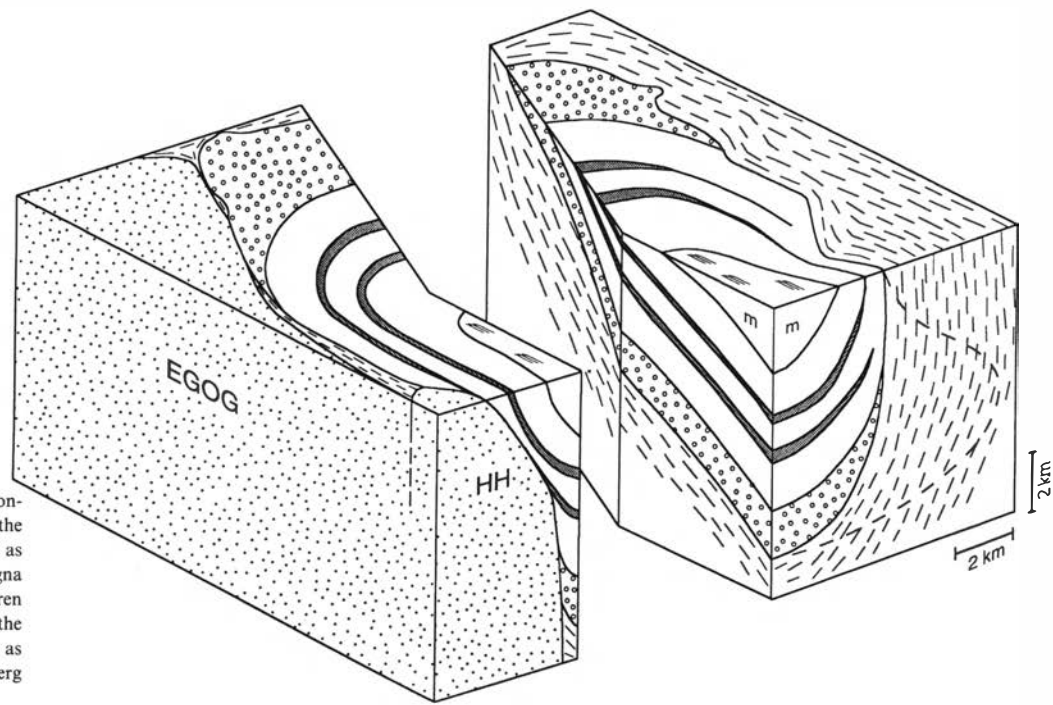


Fig. 6. Block diagram demonstrating the general shape of the Bjerkreim lobe. Ornamentation as in Fig. 4. EGOG: Egersund-Ogna anorthosite; HH: Håland-Helleren anorthosite. Dashed line marks the outline of the BKS intrusion as suggested by Smithson & Ramberg (1979).

merous and closely related to the intensity of the L<sub>1</sub>/S<sub>1</sub> fabric observed in the field. Plagioclase, which is the dominant mineral in most rocks, and to a minor extent olivine, have recrystallized to a grain size of ca. 500 μm (Fig. 2D). A transition from weakly recrystallized rocks with dominantly igneous texture through more intensely

recrystallized rocks with porphyroclastic texture, to completely recrystallized rocks with granoblastic texture is observed with increasing intensity of L<sub>1</sub>/S<sub>1</sub>. Thus the most intensely recrystallized rocks are found in the limbs, whereas the best preserved igneous textures are found in the lower part of the hinge zone. No major

Fig. 4. Geometry of the fabric elements S<sub>1</sub> and L<sub>1</sub> presented in lower hemisphere stereographic projections. Each projection refers to one of nine subareas in the Bjerkreim lobe. Contours: 1, 3, 5, 7, 9, etc., times uniform distribution. MV = Mean Vector (average orientation of L<sub>1</sub>). Circle ornaments: anorthosite; shading: troctolite units; m: (quartz-)mangerite; dash-dot-dash: fault or shear zone; dots: shear zone; B: Bjerkreim; H: Helleland; E: Lake Eptelandsvatnet; T: Lake Teksevatnet; He: Hettebøknuten; Te: Terland; G: Gyrhesten; St: Storknuten; HI: Lake Hellersvatnet; S: Slettebø; Ge: Geiterås. The Helleland fault is along the boundary between subareas 3, 4, and 5 towards the NW and 6, 7, and 8 towards the SE.



Fig. 7. Norite from the southern limb at Geiterås (Fig. 4; UTM 35.0/88.6). Modal layering ( $S_0$ ) horizontal and foliation ( $S_1$ ) parallel to pencil. Looking southwest.



Fig. 9. Leucotroctolite from the southern limb at Storeknuten (Fig. 4; UTM 34.3/90.7), displaying ellipsoidal olivines (dark), some of which are partly transformed to other mafic minerals. Lineation approximately parallel to pen.

change in mineralogy is associated with the recrystallization. This is ascribed to a dominantly dry environment (granulite facies) during deformation.

### Estimate of strain state

The intensity of the fabric and the degree of recrystallization may be taken as first order indications of the strain state. The lack of ideal 'strain markers' means that the exact amount of strain is generally difficult to estimate. However, the two troctolite units (Fig. 4) offer certain possibilities in this respect. Olivine occurs as dispersed grains of 0.5–1 cm size which appear in the field to be approximately spherical in rocks with weak fabrics and ellipsoidal in rocks with more intense fabrics (Fig. 9).

The shape of these grains is therefore assumed to reflect the amount of strain in the surrounding rocks.

The applicability of the olivine grains as strain markers depends mainly on two criteria:

(1) *The shape of the grains must be statistically spherical in undeformed rocks.* This criterion is only partly fulfilled. Although the grains are seen as spheres on weathered surfaces, they display irregular, angular shapes in thin section. Some grains have aspect ratios of up to 1.5, which suggests that the total strain calculated from the shape of deformed grains in some cases are maximum values. However, the majority of relatively undeformed grains approximate to spherical shapes. It is therefore assumed that possible deviations from original sphericity result in only small errors in the calculated strain.

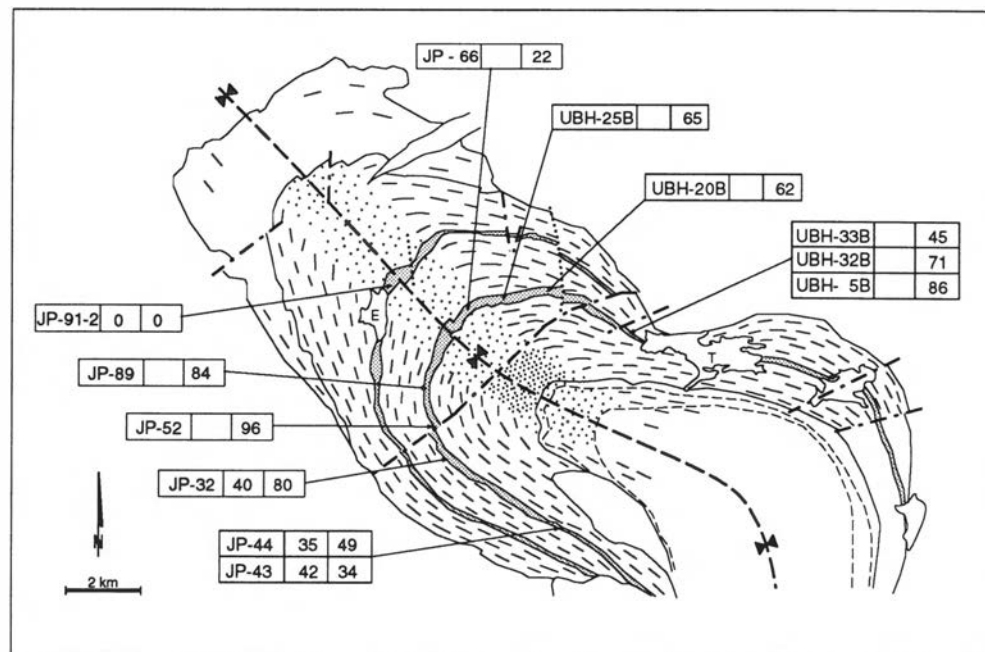


Fig. 8. Gross regional variation in fabric type in the Bjerkreim lobe: Dash: L/S-tectonite; dot: L-tectonite. Variation of strain as calculated from olivine grains or aggregates. Left box: Specimen identification; middle box: percent flattening; right box: percent extension; Empty middle box means that the strain is of constrictional type. For other information: see Fig. 4.



(2) *The olivine and the surrounding plagioclase-dominated matrix must have comparable rheological properties.* Laboratory experiments indicate that the strength of single grains of olivine would be several orders of magnitude higher than the strength of a plagioclase-dominated matrix (e.g. Carter & Tsenn 1987). However, several factors complicate the situation. The olivines often do not occur as single grains but as complex aggregates of olivine, orthopyroxene and Fe-Ti oxides with minor hornblende and biotite, formed by the breakdown of primary olivine (e.g. Barton & van Gaans 1988; Barton et al. 1991; Nielsen & Wilson 1991). The microstructures of the reaction products show that the reaction took place prior to or contemporaneously with the deformation. Obviously the rheological properties of these aggregates are very difficult to predict. However, in deformed rocks from one particular locality the shapes of aggregates are not significantly different from the shapes of unaltered olivine grains. We therefore conclude that the rheology of aggregates and that of single grains are comparable.

The presence of hornblende and biotite in the reaction aggregates indicates that although the environment was generally dry, some hydrous fluids may have been present in the vicinity of the deforming olivine grains. This may have acted as a softening factor, as shown by, e.g., Chopra & Paterson (1984) and Mackwell et al. (1985), and thus brought the rheology of the markers closer to that of the matrix. Furthermore, the matrix is not composed of pure plagioclase but contains a certain amount of Fe-Ti oxide grains (e.g. Fig. 2D). Comparison with the properties of pure anorthosite (Carter & Tsenn 1987) is therefore uncertain. It is known that a dispersed foreign phase may result in increased creep strength of the aggregate as a whole (e.g. Anderson et al. 1990). This could therefore further decrease the rheological difference between matrix and marker. However, it seems unlikely that the difference of several orders of magnitude is reduced to zero.

These theoretical considerations led us to conclude that the strain values, calculated on the basis of olivine grain shapes, most likely represent *minimum* estimates.

The dimensions of olivine grains and aggregates were measured in 12 specimens from locations shown in Fig. 8 (see Appendix). Two thin sections were prepared in each case, one parallel to the lineation and perpendicular to the foliation and one perpendicular to both foliation and lineation. If a preferred orientation of the grains/aggregates was observed, the dimensions of the grains were measured and the aspect ratio calculated. For sections parallel to the lineation this value is assumed to correspond to  $S_1/S_3$ , and in sections perpendicular to the lineation to  $S_2/S_3$ , where  $S_1$ ,  $S_2$  and  $S_3$  are the long, intermediate and short dimensions of the strain ellipsoid. If a preferred orientation could not be observed, either in hand specimen or in thin section, aspect ratios larger than 1 were assumed to result from primary igneous variations in shape and they were not used in the strain calculation. The strain was calculated as engineering

strain  $\Delta S/S_0$ , where  $S_0$  is the diameter of the originally spherical strain ellipsoid. The values are presented as total extension ( $e_1$  in %) parallel to  $L_1$  and flattening ( $e_3$  in %) perpendicular to  $S_1$ . Where no foliation is observed, only the value of extension is indicated.

The value of the flattening component increases fairly abruptly (apparently at the Helleland fault) from the area of pure extension in the hinge zone to the area of flattening in the southern limb, where it appears to have a fairly constant value. In the northern limb pure L-tectonites are observed from the hinge zone to the area west of Lake Teksevatnet. If the relatively low value of extension of specimen UBH-33B (based on only two markers) is disregarded the values reflect increasing strain, which is also suggested by increasing fabric intensity towards the limb.

If the calculated values of strain are taken to represent the strain of both the troctolitic and surrounding leuconoritic rocks, a predeformation thickness of major igneous units can be estimated. It is found that the layers between the anorthosite and the upper troctolite unit generally have a constant thickness throughout the area, whereas from the level of the upper troctolite unit and towards the mangerites an increasing thickness difference is observed, mainly between the northern limb and the rest of the lobe.

## Monzonoritic dykes

A series of generally monzonoritic dykes, known as the Lomland dyke system (Duchesne et al. 1985; Nielsen & Wilson 1991) crosscuts the hinge zone of the syncline (Fig. 1). With the exception of one dyke which is affected by a minor shear zone (see below), they appear to be unaffected by solid state deformation. Numerous xenoliths of foliated and lineated rocks which clearly belong to the BKSJ intrusion are observed in the dykes. The fabric of the xenoliths is commonly rotated relative to that of the adjacent layered rocks, which shows that the major phase of deformation that affected the intrusion had ceased at the time of intrusion of the dyke system.

## Minor shear zones

Shear zones overprint the  $L_1/S_1$  fabric at several localities. The dominant strike of the shear zones is north to northwest with a westerly dip of 30–40°, although dips towards the east are also observed. The majority of the shear zones are a few centimetres wide and cause an equally small displacement. However, wider shear zones are observed in a few places (Fig. 4). One example is in the northeastern limb near Terland (Fig. 4; UTM 37.5/95.2), where a shear zone of at least 2 km length and 10–20 cm width displaces the igneous layering about 200 m with a dextral sense. In the hinge zone northeast of Lake Eptelandsvatnet (Fig. 4; UTM 33.2/96.5) a shear

zone several metres wide is observed in one of the numerous Lomland dykes. As this shear zone runs parallel to the orientation of the dyke it is not possible to determine the displacement across the zone. In several minor (cm-scale) dykes shear zones are observed parallel to the dyke walls, and a shear zone about 30–40 cm wide forms the margin of an approximately 100-m-thick monzonitic dyke in the hinge zone near Gyrhesten (Fig. 4; UTM 34.5/93.9). This suggests that the dykes and their immediate surroundings were rheologically weaker than the BKSK intrusion itself during the shearing event, and consequently acted as loci for the formation of shear zones.

The shear zones are commonly associated with a recrystallization-induced grain size reduction from about 500  $\mu\text{m}$  in the unsheared rocks to 10–50  $\mu\text{m}$  in the shear zones. No introduction of new mineral phases is observed, although in one case the amount of amphibole is increased considerably at the expense of pyroxene. This indicates that formation of the shear zones took place while the area was still under granulite facies conditions.

### Late brittle structures

Brittle structures in the area include a series of faults and numerous joints and fractures. Faults occur throughout the area, although most dominantly in the northwestern part. They are generally steep normal faults with a displacement ranging from a few centimetres to a few metres. Mapping of igneous units reveals displacements of several hundred metres at certain locations, e.g. across the Helleland fault (Fig. 4), but these displacements are usually located in rivers and streams or covered by Quaternary deposits so that it has not been possible to determine their status as faults or shear zones.

Fault surfaces in leuconoritic rocks commonly display a thin film of fine-grained, low-grade metamorphic minerals such as chlorite and talc, whereas faulting of anorthosite seems to be related only to sericitization of the plagioclase. This indicates that faulting was accompanied by a minor influx of hydrous fluids which did not carry a significant amount of externally derived material.

Joints occur in the entire area, commonly in sets of two dominant orientations which may result in a 'brick wall'-like appearance of the rocks. This structure is locally accompanied by intense fracturing of minerals on a thin section scale.

### Discussion

#### *Origin and significance of $L_1/S_1$ fabrics*

Any model of the structural development of the BKSK intrusion is critically dependent on whether the  $L_1/S_1$  fabric is interpreted as a result of solid state deformation of the rocks, or if some fabric is assumed to have been present in the rocks prior to the onset of deformation.

Such pre-tectonic fabrics may result from igneous flow processes or compaction of an unsolidified crystal mush (e.g. Nicolas 1992). Owing to the general parallelism between fabric and layering, the fabric has previously been interpreted as largely an igneous feature of the rocks, and designated 'igneous lamination' by, e.g., Michot (1960, 1965) and Duchesne (1987), whereas Nielsen & Wilson (1991) and Jensen et al. (1993) regarded it as locally igneous and locally tectonic.

Although we have observed some examples of rocks in which the foliation is defined by an alignment of plagioclase laths which is unmistakably of igneous origin, the observed fabric is generally defined by mafic minerals in a matrix of partly or totally recrystallized plagioclase, which makes it difficult to distinguish directly between primary and secondary fabrics. The distinction must therefore be a matter of interpretation.

The leuconorites of the lower part of the hinge zone (subarea 4) which contain the best preserved igneous textures generally show no foliation. Therefore the only possible pre-tectonic fabric of this area is a weak lineation. The lack of lineation in the lower troctolite unit is an indication that the present lineation in the leuconorites is in fact entirely pre-tectonic. In the outer limbs (subareas 6 and 9) where the  $L_1/S_1$ -fabric is extensively developed together with granoblastic metamorphic textures, concordant fabrics in both country rock and gneissic xenoliths demonstrate that the fabric in these areas is dominantly a deformational feature. Any pre-tectonic fabrics in these areas have been completely obscured by the recrystallization. The remaining problem is thus how to interpret the fabrics observed in the partly recrystallized rocks of the areas between the hinge and the outer limbs. In these areas the troctolites generally have an L-type of fabric whereas the leuconorites have an L/S-fabric. This suggests that the observed foliation is largely pre-tectonic and absent in the troctolites due to a difference in igneous processes, whereas the lineation is the result of deformation which has affected both rock types. On the other hand, the close association between the degree of recrystallization and the intensity of both fabric elements indicates that they are both of tectonic origin. The only model that explains both of these observations is one in which a pre-tectonic lamination generally existed in the leuconoritic rocks but gradually decreased in intensity towards the present hinge zone. This, in turn, suggests that the lamination developed during crystallization of the leuconorites (as opposed to later compaction caused by the weight of overlying cumulates which would also have affected the troctolites) and that a slight trough-shape existed throughout crystallization of the layered series. This caused the partly crystalline mush at the top of the pile of magmatic cumulates to flow towards the hinge of the trough, thereby aligning the crystallizing grains in the flow plane (Fig. 10A). However, the constant pre-deformation thickness of igneous units in the lower part of the series shows that the dip towards the hinge zone may initially have been of the

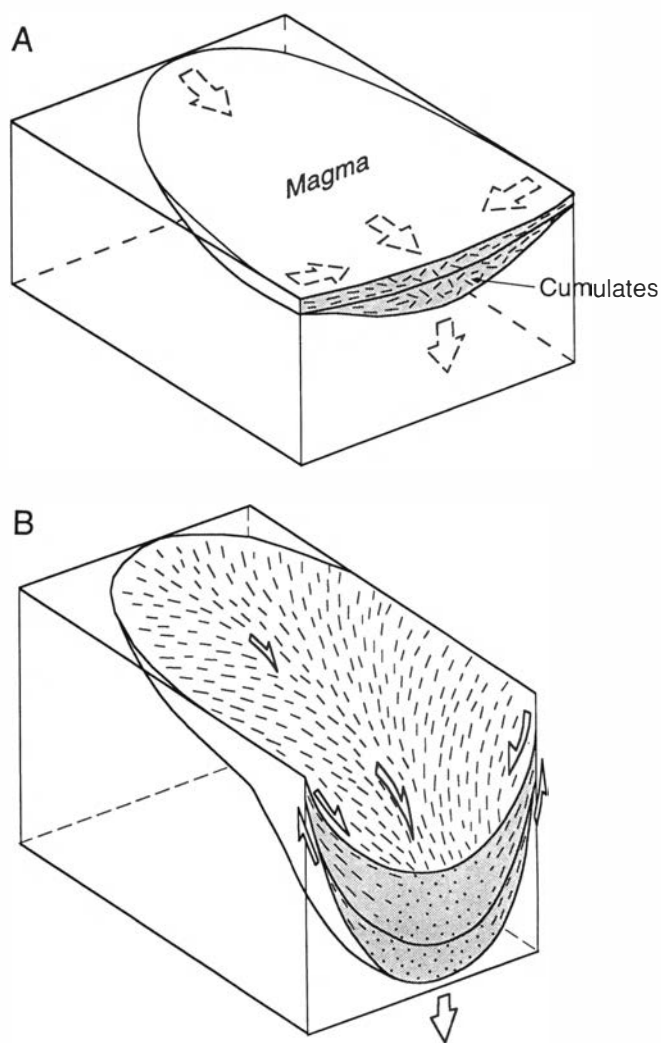


Fig. 10. Schematic block diagrams, illustrating the suggested model of tectonic evolution of the Bjerkreim lobe. A: The magmatic stage. Subsidence of the magma chamber leads to flow of the unsolidified material along the chamber floor, forming igneous lamination along the limbs. Some compaction of the underlying cumulates may intensify lamination. B: Deformation in the solid state. Simple shear-like flow along the limbs and convergent flow in the centre forms L/S- and L-tectonites respectively. See text for further explanation.

order of  $1^\circ$  or less. The lack of lamination in the troctolites may be explained in terms of a relatively rapid crystallization of these units (Nielsen & Wilson 1991).

The overprinting solid state deformation increased the intensity of the planar fabric in the leuconorites, whereas the lack of foliation in the troctolites suggests either that the deformation tended to concentrate in the rocks that already contained a planar fabric, or that the strain was homogeneous but only sufficiently large to form a distinct foliation in rocks with a previous lamination.

#### State of strain

Because of the above considerations it is assumed that the observed foliation and lineation generally reflect flattening and constrictional types of strain respectively. The quantitative values of the strain of any leuconoritic rock may be inferred by comparing the intensity of the fabric

to that of the leuconoritic rocks immediately surrounding the troctolite units for which strain analysis has been performed. In general, the gradient in strain from the lower to the higher troctolite unit in the hinge zone (0–22%; Fig. 8) continues in the leuconoritic rocks, as shown by the increasing intensity of the lineation. A conservative estimate is a few percent elongation in the leuconorites of subarea 4 and a considerably higher value (possibly of the order of 100–150% elongation) in the norites of subarea 7. In the limbs the value of the strain appears to be fairly constant from the base to the top of the layered series. The values may be somewhat higher than those of the troctolites as shown by the more intense fabrics. In the northern limb the prominent foliation of the leuconorites shows that these rocks have been flattened, although this is not indicated by the olivines in the troctolite units, as discussed above. No markers are available for the mangerites and quartz-mangerites, but the considerably lower intensity of the fabrics suggests that the strain is lower than in the underlying layered rocks.

#### Models of syncline development

A simple interpretation of the observed structures is a model in which an original almost horizontal layering with a concordant foliation is folded with contemporaneous shortening across the axial surface, leading to an intensified foliation in the limbs and L-tectonites parallel to the fold axis in the hinge area. This corresponds to a model suggested for the Ragno–Randa antiform of the Monte Rosa zone at Beura, Italy, in which the same pattern of L-tectonites in the hinge and L/S-tectonites in the limbs is observed (Reinhardt 1966; Milnes et al. 1981). In the case of the BKSK intrusion the original foliation may have been either an igneous lamination or a tectonic foliation formed by an earlier phase of deformation. However, if this model is applied, the amount of shortening (incremental strain) in the hinge area would be expected roughly to resemble that of the limbs, which would be reflected by comparable intensities of microstructural deformation and recrystallization. This is inconsistent with the observed gradient from almost unaltered igneous textures to completely recrystallized textures from hinge to limbs. Likewise, it does not explain the gradient in lineation intensity from the lower to the higher part of the hinge zone or the convergence of lineations observed especially in the northern limb. We find that as all the observed deformational features are closely linked to the shape of the syncline, they probably reflect a single phase of deformation which was intense in the limbs and the upper part of the layered rocks of the hinge zone and less intense in the lower hinge zone and the mangerites. The convergence of the lineations (Fig. 3B) indicates that this deformation had the character of a passive gravity-induced subsidence rather than a phase of cylindrical folding. The centre of convergence of the

lineations is located beneath the quartz-mangeritic rocks south of Lake Teksevatnet in the southeastern part of the area, which causes the lineations to be roughly parallel to the fold axis in the major part of the area. However, the synclinal shape of the intrusion shows that the deformation was not just a simple 'inverted diapirism' centred around this point, but rather had the geometry of an elongate trough which subsided faster in the area beneath the mangeritic rocks than in the area further northwest (Fig. 10B). If this model is applied, the local orientation of the lineation represents the direction of (incremental) mass flow. The observed Fe-Ti oxide pressure shadows (Fig. 2D) parallel to the lineation support this interpretation of the lineation and confirm that the motion was (at least locally) non-coaxial. Because of the difference in the rate of subsidence between the north-western and the southeastern parts the trough may have developed a slight cone shape which caused the solid state flow paths to converge, especially in the central part of the syncline. This type of flow pattern may result in a strongly prolate strain ellipsoid and the formation of L-tectonites as illustrated by, e.g., Twiss & Moores (1992). Along the limbs the flow had a component of shear subparallel to the original layering which led to the formation of L/S-tectonites and locally an angle between  $S_0$  and  $S_1$ . The shear direction was generally towards the fastest subsiding centre. However, in some areas towards the northwest where the viscous drag towards this point was smaller it may locally have been orientated towards the hinge of the syncline instead, which led to a rotation of the lineations as is the case in subareas 3 and 4 (Figs. 3 and 4).

It is noteworthy that the pattern of pure L-tectonites in the centre of the syncline, grading into L/S-tectonites along the limbs, resembles the pattern produced in several laboratory scale models of gravitationally subsiding troughs or inverted diapirs (Dixon & Summers 1983; Cruden 1990). Furthermore, LeBlanc et al. (1994) recently described a remarkably similar pattern which they interpreted as a result of magma flow in a series of diapirically emplaced granitic bodies. These observations strongly support the interpretation that the deformation was a process of passive vertical movement, probably induced by gravitational instabilities in the area.

The subsidence process was probably initiated during crystallization of the lower anorthositic rocks or very early during the formation of the layered series as shown by the interpreted presence of igneous lamination in the rocks away from the present hinge zone. Thus the igneous flow may be regarded as the earliest stage of a continuous process which gradually shifted to plastic deformation as the amount of crystallized grains became sufficiently high to form a stress supporting network. This interpretation explains why igneous lamination appears to have formed preferably in rocks which have also been affected by relatively intense solid state deformation.

The low intensity of the fabric in the mangeritic and quartz-mangeritic rocks may be taken as an indication

that these rocks intruded at a late stage during deformation. However, as the shift in fabric intensity appears to be gradual, we consider it more likely that they experienced most of the deformation along with the rest of the intrusion, but that the relatively low density of the quartz-mangerites compared to that of the noritic rocks caused them to 'float' more or less passively during the subsidence. In a series of multi-layer experiments Dixon & Summers (1983) found that a layer of a given density does in fact subside more slowly than underlying denser material.

The rocks of the lower anorthositic part of the intrusion probably had a density even closer to that of the country rock than the quartz-mangerites. However, as the anorthositic rocks lie under the deforming leuconorites they could not have been completely unaffected by the deformation. The low intensity of deformation observed in the exposed parts of this unit is therefore more easily explained in terms of its distance from the quickest subsiding centre. As the gravity measurements did not allow Smithson & Ramberg (1979) to differentiate between anorthosites and felsic gneisses no information is available about the quantity of this type of rock at deeper levels, and the extent of its development (e.g. in Fig. 6) is a matter of interpretation.

Some lineations in the southern limb (subarea 6) display orientations that deviate from the general convergent pattern. This perhaps suggests that another quickly subsiding area was located further southeast towards the Sokndal lobe which most likely represents the other half of the trough structure. However, it is clear from the strain analysis that the strain pattern in the southern limb is generally atypical of the area as a whole, as shown by the larger component of flattening strain. This may be related to the proximity of the large massif type anorthositic bodies to the west of the intrusion (Fig. 6). If the updoming of the Egersund-Ogna body was more or less contemporaneous with the subsidence of the BKSK intrusion, it may have caused a considerable amount of flattening strain along the southern limb. It seems likely that the vertical movements, caused by gravitational instabilities in the area, were more or less contemporaneous since transfer of mass from deeper to higher levels of the crust must be accompanied by a transfer of mass in the opposite direction in order to maintain mass balance.

Whether the subsidence of the BKSK intrusion was 'active', in the sense that the major driving force was a density contrast between the intrusion and the surrounding gneisses or 'passive', in the sense that the major driving force was either the uprise of massif type anorthosites or possibly a phase of contemporaneous folding in the country rock, is difficult to determine on the basis of the field evidence. Smithson & Ramberg (1979) found that the layered rocks are associated with a large positive gravity anomaly relative to the surrounding gneisses and anorthosites. Thus it is possible that the density of these rocks was the dominant driving force. If the interpretation of the above authors is followed, the

shape of the intrusion below the present level of erosion resembles an inverted diapir to a larger extent that is visible at the surface (Fig. 6), indicating that the process was in fact due to the density of the intrusion itself. On the other hand, the development of the syncline appears to have been initiated very early during crystallization, at a time when the pile of dense rocks was not likely to have been thick enough to exert a stress exceeding the flow stress of the country rock. The massif type anorthosites are volumetrically far in excess of the leuconorites, which means that doming must have led to a considerable mass deficiency at depth, which, in turn, must have been balanced by the sinking of a large amount of material in their vicinity. The BSKS intrusion may have sunk more easily than the charnockitic gneisses because of its higher density. Furthermore, the vertical movements of the intrusive bodies may have been accompanied by contemporaneous orogenic shortening, leading to the large gentle folds in the gneisses to the northeast of the intrusives observed by Hermans et al. (1975).

If the density of the intrusion in itself was sufficient to initiate the subsidence process, a similar process might occur in many other comparable environments. However, very few examples of similar structures have been described. Although a great number of mafic intrusions have a synclinal or funnel shape, most of these do not show the prominent tectonic fabric and microstructure observed in the BSKS intrusion. In the case of mafic intrusions deformed in the solid state, the authors have no knowledge of examples of similar patterns of prominent, converging lineations. However, Robins (1982) and Bennett et al. (1986) described a series of mafic and ultramafic bodies in the Seiland area, North Norway which, like the BSKS intrusion, have a synclinal shape with a post-magmatic layer-parallel foliation. These intrusions may have been deformed by a process similar to the one suggested here for the BSKS intrusion. It may be that although gravitational subsidence is a potential mode of deformation of many mafic intrusive rocks, the process needs to be triggered by some external factor, which in the case of the BSKS intrusion could have been the movement of neighbouring rocks or a phase of orogenic shortening.

The recent datings of Duchesne et al. (1993) of anorthosites and monzonorites yield a relatively narrow time-span (~10 Ma) between the crystallization of these two rock types. This is also the maximum time-span for both crystallization and deformation of the BSKS intrusion. This is consistent with our interpretation that the magmatic and solid state processes were closely linked.

## Summary and conclusions

The crystallization and deformation history of the Bjerkreim lobe of the BSKS intrusion can be summarized as follows:

1. Intrusion of magma into a broad saucer-shaped chamber. Slight curvature of the chamber floor caused lamination to form, preferably in the areas away from the centre. The curvature may have resulted from regional synmagmatic folding. Subsidence of the magma chamber floor accelerated during the crystallization of the layered series.
2. Continued subsidence in the solid state led to the formation of tectonic fabrics ( $L_1/S_1$ ) and recrystallization of primary igneous minerals. The subsidence was quicker in the southeastern end of the syncline, which caused material to flow towards this centre, forming a distinct tectonic lineation. Contemporaneous shear along the limbs of the developing syncline gave rise to a foliation, roughly parallel to layering and preferably in rocks that already contained a planar lamination. A relatively large amount of flattening strain along the southern limb may have been caused by contemporaneous updoming of the neighbouring Egersund–Ogna massif anorthosite. The entire process may have been accompanied by (continued) regional folding which eventually led to the formation of an isoclinal syncline. The mangeritic and quartz-mangeritic rocks may have been emplaced towards the end of the deformation and therefore developed a less intense fabric. However, it is equally possible that they experienced most or all of the deformation, but were relatively unaffected because of their low density.
3. When deformation had ceased, the area was intruded by a series of monzonoritic dykes (the Lomland dyke system).
4. Both leuconorites and monzonorites were affected by minor shear zones which appear to have formed preferably in the monzonorites or at leuconorite/monzonorite contacts. This event took place while the rocks were still under granulite facies conditions.
5. The area was affected by late brittle faulting and fracturing under low-grade conditions.

*Acknowledgements.* – We thank J. R. Wilson, B. Robins and referees A. G. Milnes, C. Talbot and J. C. Duchesne for constructive criticism of the manuscript. Technical assistance was received from L. Jans and J. Kjeldsen.

Manuscript received September 1993

## References

- Anderson, J. C., Leaver, K. D., Rawlings, R. D. & Alexander, J. M. 1990: *Materials Science*, 608 pp. Chapman and Hall, London.
- Barton, M. & van Gaans, C. 1988: Formation of orthopyroxene-Fe-Ti oxide symplectites in Precambrian intrusives, Rogaland, southwestern Norway. *American Mineralogist* 73, 1046–1059.
- Barton, M., Sheets, J. M., Lee, W. E. & van Gaans, C. 1991: Occurrence of low-Ca clinopyroxene and the role of deformation in the formation of pyroxene-Fe-Ti oxide symplectites. *Contributions to Mineralogy and Petrology* 108, 181–195.
- Bennett, M. C., Emblin, S. R., Robins, B. & Yeo, W. J. A. 1986: High-temperature ultramafic complexes in the North Norwegian Caledonides: I – Regional setting and field relationships. *Norges geologiske undersøkelse* 405, 1–40.
- Carter, N. L. & Tsenn, M. C. 1987: Flow properties of continental lithosphere. *Tectonophysics* 136, 27–63.



- Chopra, P. N. & Paterson, M. S. 1984: The role of water in deformation of dunite. *Journal of Geophysical Research* 89, 7861–7876.
- Cruden, A. R. 1990: Flow and fabric development during the diapiric rise of magma. *Journal of Geology* 98, 681–698.
- Dixon, J. M. & Summers, J. M. 1983: Patterns of total and incremental strain in subsiding troughs: experimental centrifuge models of inter-diapir synclines. *Canadian Journal of Earth Science* 20, 1843–1861.
- Duchesne, J. C. 1987: The Bjerkreim–Sokndal massif. In Majier, C., Padget, P. (eds): The geology of southernmost Norway: an excursion guide. *Norges geologiske undersøkelse, Special Publication 1*, 56–59.
- Duchesne, J. C., Demaiffe, D., Roelandts, I. & Weis, D. 1985: Petrology of monzonitic dykes in the Egersund–Ogna anorthosite (Rogaland, SW Norway): trace elements and isotopic constraints. *Contributions to Mineralogy and Petrology* 90, 214–225.
- Duchesne, J. C. & Hertogen, J. 1988: Le magma parental du lopolithe de Bjerkreim–Sokndal (Norvège méridionale). *Comptes Rendus de L'Académie des Sciences Paris* 306, 45–48.
- Duchesne, J. C., Schärer, U. & Wilmart, E. 1993: A 10 Ma period of emplacement for the Rogaland anorthosites, Norway: evidence from U–Pb ages. *Terra abstracts. Supplement No. 1 to Terra nova* 5, p. 64.
- Hermans, G. A. E. M., Tobi, A. C., Poorter, R. P. E. & Majier, C. 1975: The high-grade metamorphic Precambrian of the Sirdal–Ørdsdal area, Rogaland/Vest-Agder, southwest Norway. *Norges geologiske undersøkelse* 318, 51–74.
- Jensen, J. C., Nielsen, F. M., Duchesne, J. C., Demaiffe, D. & Wilson, J. R. 1993: Magma influx and mixing in the Bjerkreim–Sokndal layered intrusion, South Norway: evidence from the boundary between two megacyclic units at Storeknuten. *Lithos* 29, 311–325.
- Leblanc, D., Gleizes, G., Lospinasse, P., Olivier, Ph. & Bouchez, J.-L. 1994: The Maladeta granite polydiapir, Spanish Pyrenees: a detailed magneto-structural study. *Journal of Structural Geology* 16/2, 223–235.
- Mackwell, S. J., Kohlstedt, D. L. & Paterson, M. S. 1985: The role of water in the deformation of olivine single crystals. *Journal of Geophysical Research* 90/B13, 11319–11333.
- Majier, C. & Padget, P. 1987: The geology of southernmost Norway: An excursion guide. *Norges geologiske undersøkelse, Special Publication 1*, 109 pp.
- Majier, C. 1987: The metamorphic envelope of the Rogaland intrusive complex. In Majier, C. & Padget, P. (eds): The geology of southernmost Norway: An excursion guide. *Norges geologiske undersøkelse, Special Publication 1*, 68–73.
- Michot, P. 1960: La géologie de la catazone: Le problème des anorthosites, la paléogénèse basique et la tectonique catazonale (Norvège Méridionale). *International Geological Congress Norden, Guidebook A9*, 147–173.
- Michot, P. 1965: Le magma plagioclasiue. *Geologische Rundschau* 55, 956–976.
- Michot, J. & Michot, P. 1969: The problem of the anorthosites. The South Rogaland igneous complex (southwestern Norway). In Isachsen, Y. W. (ed.): Origin of anorthosites and related rocks. *New York State Museum and Science Service, Memoir 18*, 399–410.
- Milnes, A. G., Grellier, M. & Müller, R. 1981: Sequence and style of major post-nappe structures, Simplon-Pennine Alps. *Journal of Structural Geology* 3/4, 411–420.
- Nicolas, A. 1992: Kinematics in magmatic rocks with special reference to gabbros. *Journal of Petrology* 33/4, 891–915.
- Nielsen, F. M. 1992: Magmakammerprocesser, belyst med udgangspunkt i Bjerkreim–Sokndal intrusionen, Rogaland, Sydnorge. Thesis, Aarhus University, 117 pp.
- Nielsen, F. M. & Wilson, J. R. 1991: Crystallization processes in the Bjerkreim–Sokndal layered intrusion, south Norway: evidence from the boundary between two macrocyclic units. *Contributions to Mineralogy and Petrology* 107, 403–414.
- Pasteels, P., Demaiffe, D. & Michot, J. 1979: U–Pb and Rb–Sr geochronology of the eastern part of the south Rogaland igneous complex, southern Norway. *Lithos* 12, 199–208.
- Reinhardt, B. 1966: Geologie und Petrographie der Monte Rosa-Zone, der Sesia-Zone und der Canavese im Gebiet zwischen Valle d'Ossola und Valle Loana. *Schweizerische Mineralogische und Petrographische Mitteilungen* 46/2, 553–678.
- Robins, B. 1982: The geology and petrology of the Rognsund Intrusion, West Finnmark, Norway. *Norges geologiske undersøkelse* 371, 1–55.
- Smithson, S. B. & Ramberg, I. B. 1979: Gravity interpretation of the Egersund anorthosite complex, Norway: Its petrological and geothermal significance. *Geological Society of America Bulletin* 1/90, 199–204.
- Twiss, R. J. & Moores, E. M. 1992: *Structural Geology*, 532 pp. W. H. Freeman & Co., New York.
- Verstevee, A. J. 1975: Isotope geochronology in the high-grade metamorphic Precambrian of southwestern Norway. *Norges geologiske undersøkelse* 318, 1–50.
- Wielens, J. B. W., Andriessen, P. A. M., Boelrijk, N. A. I. M., Hebeda, E. H., Priem, H. N. A., Verduermen, E. A. T. & Verschure, R. H. 1980: Isotope geochronology in the high-grade metamorphic Precambrian of southwestern Norway: new data and reinterpretations. *Norges geologiske undersøkelse* 359, 1–30.
- Wilmart, E. & Duchesne, J. C. 1987: Geothermobarometry of igneous and metamorphic rocks around the Åna-Sira anorthosite massif: Implications for the depth of emplacement of the South Norwegian anorthosites. *Norsk Geologisk Tidsskrift* 67/3, 185–196.

## Appendix

Total strain as calculated on the basis of deformed olivine grains (single grains), aggregates of recrystallized grains and olivine/orthopyroxene/oxide aggregates.

Specimen	Locality (UTM-coordinates)	Type or marker	Number of markers		Mean aspect ratio of markers		Flattening $\epsilon_3$ (%)	Extension $\epsilon_1$ (%)
			Section $\perp$ to lineation	Section $\parallel$ to lineation	X	Y		
JP-43	Svartevatnet (37.6/88.7)	Single grains	6	2	2.20	2.30	42	34
JP-44	Svartevatnet	Aggregates	5	4	1.60	2.30	35	49
JP-32	Storknuten (34.4/90.7)	Single grains	3	2	1.50	2.95	40	80
JP-52	Helleland (33.9/91.9)	Aggregates		7	n.p.p.	2.70		96
JP-89	Erretjørn (33.6/92.8)	Aggregates		3	n.p.o.	2.50		84
JP-66	Benkafjellet (34.8/94.8)	Aggregates		4	n.p.o.	1.35		22
UBH-25 B	Hettebøknuten (35.5/95.7)	Single grains		5	n.p.o.	2.12		65
UBH-20 B	Terland (38.5/95.5)	Aggregates		3	n.p.o.	2.07		62
UBH-32 B	Teksevatnet (39.8/93.7)	Single grains		12	n.p.o.	2.06		71
UBH-33 B	Teksevatnet	Aggregates		2	n.p.o.	1.75		45
UBH-5 B	Teksevatnet	Single grains		9	n.p.o.	2.54		86
		Aggregates						
		Recrystallized grains						
JP-91-2	Eptelandsvatnet (32.6/95.6)	Single grains			n.p.o.	n.p.o.	0	0

X = mean value of  $S_2/S_3$ , Y = mean value of  $S_1/S_3$ , where  $S_1$ ,  $S_2$  and  $S_3$  = long, intermediate and short dimension of the markers. X and Y are assumed to correspond to the aspect ratios of the strain ellipsoid of the rock. The flattening is calculated as  $(S_0 - S_3)/S_0 = (\sqrt[3]{XY} - 1)/\sqrt[3]{XY}$  and the extension as  $(S_1 - S_0)/S_0 = (Y - \sqrt[3]{XY})/\sqrt[3]{XY}$ , where  $S_0$  is the diameter of an original sphere.

n.p.o. = no preferred orientation is visible in thin section, in which case a value of 1 is used for X in the calculations.